PARAMETER
JURNAL MATEMATIKA, STATISTIKA DAN TERAPANNYA

e-ISSN. 2829-6303
Vol. 05, No. 1, April 2026
Pages 181-194

Check for updates

Improving Land Use Classification Accuracy Using Zonal Statistics And Supervised Machine Learning

I Gede Awantara[1]*, Kusman Sadik[2], Cici Suhaeni[3], Agus Mohamad Soleh[4]

[1,2,3,4] Department of Statistics and Data Science,
School of Data Science, Mathematics, and Informatics, IPB University
Dramaga Main Road, Babakan, Dramaga, Bogor Regency, 16680
West Java, Indonesia

E-mail Correspondence Author: *gedeawantara@apps.ipb.ac.id*

Abstract

This study aims to improve land use classification accuracy by integrating zonal statistics with supervised machine learning using Sentinel-2 imagery. Two classification models were developed: Model A based on single-pixel values and Model B using aggregated zonal statistics derived from polygon shapefile data. Two algorithms, Random Forest and Classification and Regression Trees (CART), were implemented and evaluated through 5-fold cross validation. The results show that Model B consistently outperformed Model A, with the best performance achieved by Random Forest Model B, reaching an overall accuracy of 73.74% and a kappa coefficient of 0.5999. Class-wise evaluation based on F1-score revealed strong performance in dominant classes such as settlement, water bodies, and rice fields, while underrepresented classes like cropland and shrubland were more difficult to classify due to class imbalance. These findings highlight the effectiveness of zonal statistics in producing more representative training features and improving model stability and accuracy in land use classification tasks.

Keywords: *Geospatial Analysis, land use classification, supervised machine learning, zonal statistics.*

: https://doi.org/10.30598/parameterv4i1pp181-194

Research Ariticle** · **Open Acces
Email: jurnalparameter@gmail.com
Homepage: https://ojs3.unpatti.ac.id/index.php/parameter

Submitted: Juny 2025
Accepted: April 2026

1. INTRODUCTION

The development of remote sensing technology and the availability of geospatial data have greatly facilitated land use classification, which was previously reliant on conventional field survey-based methods [1]. With the increased accessibility to geospatial data, such as Sentinel-2 satellite imagery, land use classification can now be performed with higher resolution and broader coverage, enabling more efficient monitoring and analysis. This classification is crucial in various fields, such as urban planning, environmental monitoring, natural resource management, and disaster mitigation [2]. One method widely used to improve the efficiency and accuracy of land classification is the application of machine learning based on geospatial data [3]. By utilizing Sentinel-2 satellite imagery as raster data and land use shapefile data as vector data, the classification process can be automated, which is expected to produce more accurate and up-to-date land use information.

Supervised machine learning is used to classify land use by leveraging vector data in the form of shapefile polygons representing land use classes as additional features to train the model. Common machine learning algorithms used in land classification from satellite imagery include Random Forest (RF) and Classification and Regression Trees (CART) [4]. These algorithms are chosen for their ability to handle multidimensional data from satellite imagery and produce classification results with high accuracy [5], [6], [7]. Although various machine learning methods have been applied in land use classification, challenges remain in optimizing the model to adapt to the complex variation in land use and improve prediction accuracy.

One key factor that affects the accuracy of land use classification is the quality of the training data used to build the machine learning model [1]. Satellite imagery is often affected by atmospheric disturbances, coordinate system differences, and variations in spatial resolution, which can lower classification accuracy [8]. To address these issues, the preprocessing phase is crucial in this study. Data preprocessing includes selecting satellite imagery with minimal cloud cover, performing radiometric and geometric corrections, and adjusting the coordinate system between the shapefile data and satellite imagery. Additionally, spectral feature extraction is conducted to enhance the quality of model input, which positively impacts classification accuracy and allows machine learning models to work more effectively [9].

The approach used to improve the quality of training data is zonal statistics. This technique allows spectral information to be extracted from Sentinel-2 imagery based on polygons in the shapefile that represent different land use classes. By using zonal statistics, the mean, maximum, minimum, and spectral variation values for each land use class can be calculated [10], [11], [12]. The application of zonal statistics enables the model to rely not only on individual pixel values, which can be noisy, but also to obtain more stable and representative information for each land use class [11].

This study focuses on improving land use classification accuracy using zonal statistics and supervised machine learning, with a case study in Tabanan Regency. This region was chosen because it has a variety of land use types, such as forests, agricultural land, urban areas, and water bodies, making it representative for testing the effectiveness of the developed model. By optimizing supervised machine learning models through shapefile data processing and spectral feature extraction from Sentinel-2 satellite imagery, this research aims to significantly improve land use classification accuracy.

It is hoped that this research will contribute to the development of land use classification methods for satellite imagery based on machine learning, which can be

applied in various scenarios, such as land change monitoring, environmental impact analysis, and natural resource management. The novelty of this study lies in the extraction of Sentinel-2 satellite image pixels using zonal statistics, which has not been widely applied in supervised machine learning-based land use classification. The results of this study are expected to provide a more effective and efficient solution for machine learning-based land use classification using geospatial data.

2. RESEARCH METHOD

2.1. Research Type

This quantitative study evaluates and compares the performance of machine learning algorithms in land use classification based on spectral features from satellite imagery, employing pixel centroid values (Model A) and zonal statistics (Model B). The data used includes Sentinel-2 Level 2A imagery and land use shapefiles, with preprocessing steps involving coordinate system adjustment and the calculation of NDVI, NDBI, and MNDWI indices. To address class imbalance, the Synthetic Minority Over-sampling Technique (SMOTE) is applied during model training to generate synthetic samples for the minority class. Two algorithms (CART and Random Forest) are trained using 5-Fold Stratified Cross Validation to ensure stable and representative performance estimation. The model evaluation is carried out using metrics such as accuracy, kappa, precision, recall, and F1-score.

2.2. Data Collection

This study utilizes Sentinel-2 Level 2A satellite imagery, which is freely available for download via https://dataspace.copernicus.eu. The dataset includes multispectral imagery with spatial resolutions of 10 meters, 20 meters, and 60 meters across 13 spectral bands relevant for land use classification **[13]**. The data selected corresponds to the year 2019, aligning with the land use shapefile data. Sentinel-2 imagery was chosen for its minimal cloud cover and relevance to the area of interest for this study. A visual example of the Sentinel-2 imagery can be seen in **Figure 1**.

Figure 1. Sentinel 2A Satellite Imagery

This study uses land use class shapefile data for Tabanan Regency, obtained from the Geospatial Information Agency, consisting of 2,167 samples representing eight land use classes. Settlement class (1,121 samples, 51.73%) and rice field class (510 samples, 23.53%) dominate the dataset, while other classes like plantation, cropland, and grassland are underrepresented. Some classes, including forest, water bodies, and shrubland, have very few samples. This imbalance, with most data concentrated in a few classes, is a critical consideration in model evaluation. To address this issue, SMOTE will be applied during model training to generate synthetic samples for the minority classes, improving the model's ability to handle the imbalance. The distribution of land use classes is shown in **Table 1**.

Table 1. Distribution of Land Use Classes and Their Proportions in Tabanan Regency

Land Use Class	Quantity	Percentage
Forest	30	1.38%
Cropland	69	3.18%
Grassland	34	1.57%
Water Bodies	30	1.38%
Plantation	332	15.32%
Settlement	1121	51.73%
Rice Field	510	23.53%
Shrubland	41	1.89%
Total	2167	100%

2.3 Preprocessing

2.3.1 Spectral Index

A spectral index is a value calculated from satellite imagery or remote sensing sensor data based on the comparison or combination of reflectance values across specific spectral bands (wavelengths) [14]. This index is used to extract specific information from the Earth's surface, such as identifying vegetation cover, water, soil, or specific land use types [15].

a. NDVI (Normalized Difference Vegetation Index)
   NDVI is a spectral index used to identify and monitor vegetation health by measuring the reflectance difference between the NIR channel (band 8, 842 nm) and the Red channel (band 4, 665 nm) [16], [14]. NDVI values range from -1 to 1, where values close to 1 indicate healthy and dense vegetation, while values close to -1 represent non-vegetated surfaces such as water or dry soil. The NDVI formula is shown in **Equation (1)**.

$$NIR - Red/NIR + Red \quad (1)$$

Commented [L1]:

b. MNDWI (Modified Normalized Difference Water Index)
   MNDWI is an index used to detect surface water, a modification of NDWI that is more sensitive and effective at distinguishing water from vegetation or soil [17]. This index uses the SWIR channel (band 11, 1610 nm) and the Green channel (band 3, 560 nm) to enhance the separation of water and vegetation [16]. The MNDWI value is calculated using **Equation (2)** [18]. MNDWI values range from -1 to 1, where values close to 1 indicate clear water, and values close to -1 represent non-water surfaces.

$$Green - SWIR/Green + SWIR \quad (2)$$

Commented [L2]: Number is black colour

c. NDBI (Normalized Difference Built-up Index)
NDBI is used to detect built-up areas in satellite imagery, distinguishing buildings and urban areas from non-urban regions. The NDBI value is calculated using the reflectance of SWIR2 (band 12, 2200 nm) and NIR (band 8, 842 nm), as shown in **Equation (3) [15]**. NDBI values range from -1 to 1, with values close to 1 indicating built-up areas and values close to -1 representing non-urban areas.

$$SWIR2 - NIR/SWIR2 + NIR \quad (3)$$

2.3.2 Zonal Statistics

During preprocessing, the coordinate reference system (CRS) of the shapefile and satellite imagery was aligned to ensure spatial consistency and avoid positional errors in classification. Zonal statistics were then used to extract features mean, maximum, minimum, and standard deviation of spectral indices within each land-use polygon as inputs for land classification models **[11]**, **[12]**. Spectral indices such as NDVI, MNDWI, and NDBI were derived from Sentinel-2 imagery to provide key information on vegetation, water, and built-up areas for land change analysis **[19]**. These index values were aggregated by zone to characterize the spatial distribution of overlapping image pixels. The resulting zonal statistics were tabulated and used as inputs for machine learning models such as CART and Random Forest offering more stable spectral representations than individual pixels and thereby improving classification accuracy **[11]**, **[12]**. The zonal statistics process is illustrated in **Figure 2**.

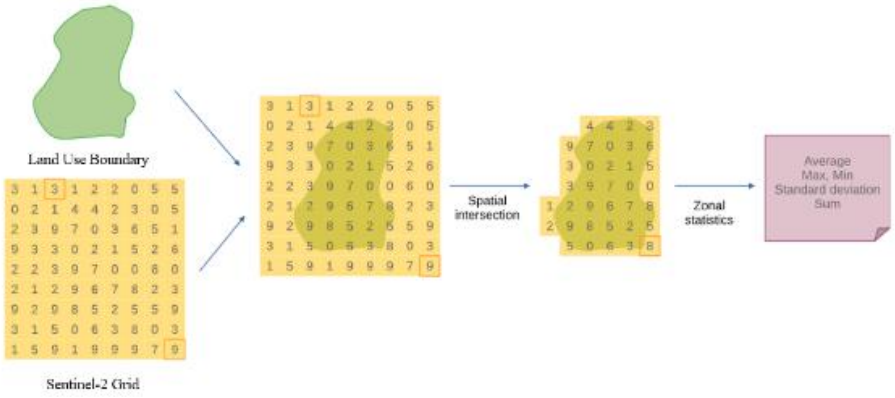

Figure 2. Spectral Extraction Process Using Zonal Statistic [12]

2.4 Analysis Methods

2.4.1 Classification and Regression Tree (CART)

CART is a decision tree based machine learning algorithm that recursively splits the data based on features that most effectively reduce impurity at each node. Feature selection and split points are determined using criteria such as Gini Impurity or Entropy, aiming to minimize impurity **[20]**. To prevent overfitting, pruning techniques are applied, either through pre-pruning or post-pruning. In this study, CART uses the Gini Impurity criterion, calculated using **Equation (4)**.

$$Gini\ (t) = 1 - \sum_{i=1}^{C} p(i|t)^2 \quad (4)$$

$Gini\ (t)$ = impurity levet at node t
C = number of classes
$p(i|t)$ = proportion of data belonging to class i at node t

2.4.2 Random Forest

Random Forest is an ensemble learning algorithm based on Classification and Regression Trees (CART) that constructs multiple decision trees using the bagging technique [21]. Each tree is trained on a random subset of both data and features, and the final prediction is obtained through majority voting. This approach reduces overfitting and improves accuracy by leveraging the diversity among trees, and it is capable of handling high-dimensional datasets. The final prediction for a sample is determined by the majority vote from all trees, as expressed in **Equation (5)**.

$$\hat{y} = majority\ vote\ \{h_1(x), h_2(x), \dots, h_b(x)\} \quad (5)$$

$\hat{y}$ = final predicton result of Random Forest
$h_b(x)$ = the b-th decision tree's prediction for input x

2.4.3 Evaluation

The evaluation of classification model performance aims to measure the accuracy and consistency of the model in assigning data to the appropriate classes. In this study, several standard evaluation metrics are used, including:

a. Overall Accuracy

Indicates the percentage of data correctly classified out of the total test data. This metric provides an overall view of model performance but can be biased when applied to imbalanced datasets. The overall accuracy is computed using **Equation (6)**.

$$Accuracy = \frac{\sum_{i=1}^{k} TP_i}{N} \quad (6)$$

where TP_i is the number of correct predictions for class i and N is the total number of test samples.

b. Kappa Coefficient

A metric that evaluates the agreement between the model's classification results and the reference data, taking into account the possibility of agreement occurring by chance. Kappa is more informative than overall accuracy, especially when dealing with imbalanced datasets. The kappa coefficient is computed using **Equation (7)**.

$$K = \frac{p_o - p_e}{1 - p_e} \quad (7)$$

where P_o is the proportion of actual agreement, and P_e is the proportion of agreement expected by chance.

c. Confusion Matrix

In multi-class classification, the confusion matrix displays the correct and incorrect predictions for each class. To calculate metrics such as precision and recall, each class is treated as the positive class while the others are considered negative. True Positive (TP) refers to samples correctly classified into the target class, False Negative (FN) are target class samples incorrectly classified into other classes, False Positive (FP) are samples from other classes wrongly classified into the target class, and True Negative (TN) are non-target class samples correctly excluded from the target class. This approach is essential for detailed evaluation, particularly when dealing with imbalanced class distributions.

d. Per Class Metrics :

- Precision: proportion of true positive predictions among all positive predictions made by the model. It indicates how accurately the model identifies relevant instances and is calculated using **Equation (8)**.

$$Precision = \frac{TP}{TP + FP} \tag{8}$$

- Recall: ratio of true positive predictions to total actual positive instances. This metric shows how well a model identifies all cases that genuinely belong to a specific class, as calculated in **Equation (9).**

$$Recall = \frac{TP}{TP + FN} \tag{9}$$

- F1-Score: calculated using **Equation (10)**, combines precision and recall through their harmonic mean and is useful for handling imbalanced data.

$$F1 = 2\frac{Recall \times Precision}{Recall + Precision} \tag{10}$$

3. RESULT AND DISCUSSION

3.1 Spectral Index Extraction

Three spectral indices NDVI, MNDWI, and NDBI were derived from Sentinel-2 Level 2A imagery to capture key land surface features: vegetation, water bodies, and built-up areas. These indices were calculated using specific band combinations as described in the methodology section, and their spatial distributions are shown in **Figure 3**.

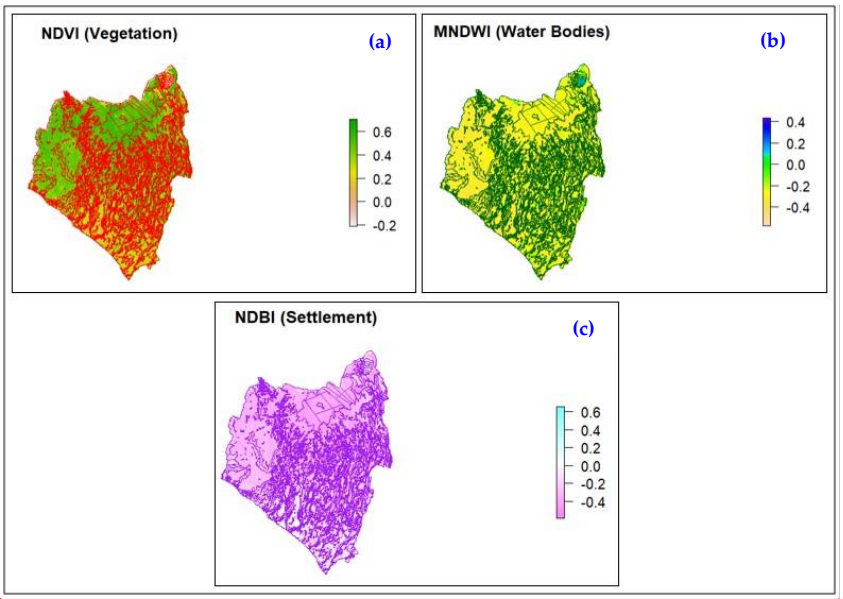

Figure 3. Spatial distribution of spectral indices in Tabanan Regency: (a) NDVI representing vegetation cover, (b) MNDWI indicating surface water presence, and (c) NDBI highlighting built up areas.

Figure 3 shows the spatial distribution of the three spectral indices across Tabanan Regency. NDVI values range from -0.2 to above 0.6, with higher values observed in the northern and northwestern areas, indicating dense vegetation cover. Lower NDVI values (below 0.2) dominate the southern and eastern regions, corresponding to built-up or barren land. MNDWI values range between -0.4 and 0.4, with higher values effectively delineating water bodies along river networks and lowland zones. NDBI values range from -0.4 to 0.4, with elevated values concentrated in the central and southern parts of the region, highlighting urbanized and developed areas. These spectral patterns confirm the effectiveness of NDVI, MNDWI, and NDBI in identifying vegetation, water bodies, and settlements, respectively. The derived index values serve as robust and discriminative features in the zonal statistics process, enhancing the reliability of input data for land use classification using machine learning models.

3.2 Summary of Spectral Index Means by Land Use Class

To capture representative spectral characteristics of different land use classes, mean values of three spectral indices NDVI, NDBI, and MNDWI were computed using the zonal statistics method. Rather than relying on individual pixel values, the mean values were aggregated over each polygon representing a specific land use class, such as forest, cropland, or built-up areas. This aggregation reduces pixel-level noise and provides a more stable input for the classification model.

Table 2. Mean Values of Spectral Indices by Land Use Class

Class	NDVI Mean	NDBI Mean	MNDWI Mean
Forest	0.4882	-0.3343	-0.3073
Cropland	0.4239	-0.2678	-0.3028
Grassland	0.2857	-0.1154	-0.2883
Water Bodies	0.1029	-0.0790	-0.0335
Plantation	0.4346	-0.2838	-0.2929
Settlement	0.2905	-0.1239	-0.2787
Rice Field	0.4466	-0.3073	-0.2820
Shrubland	0.4780	-0.3283	-0.3011

Table 2 displays the mean values of NDVI, NDBI, and MNDWI for eight land use classes, providing insight into the spectral characteristics of each category. Forest class shows the highest NDVI mean (0.4882), indicating dense, healthy vegetation with strong photosynthetic activity. Similarly, shrubland (0.4780), rice field (0.4466), and plantation (0.4346) also exhibit high NDVI values, reflecting vegetated surfaces. Cropland follows with a moderate NDVI mean (0.4239), suggesting active but less dense vegetation. In contrast, water bodies report the lowest NDVI mean (0.1029), consistent with the absence of vegetation in aquatic environments. Regarding the NDBI values, all land use classes display negative means, indicating a general lack of impervious surfaces in the study area. However, settlement and grassland classes exhibit relatively higher NDBI means (−0.1239 and −0.1154, respectively), suggesting some level of built up influence or bare soil presence. The lowest NDBI values are observed in forest (−0.3343) and shrubland (−0.3283), representing undisturbed natural areas with minimal built up infrastructure. In terms of MNDWI, water bodies stand out with the highest mean value (−0.0335), close to zero, which aligns with the expected reflectance of surface water. All other classes show more negative MNDWI values, especially forest (−0.3073), cropland (−0.3028), and shrubland (−0.3011), indicating dry conditions with limited or no water presence. Although the full zonal statistics include minimum, maximum, and standard deviation values, only the mean values are presented here for clarity and brevity**.** These spectral index summaries effectively distinguish land use types based on their spectral behavior and serve as informative features for subsequent classification modeling.

3.3 Classification Model Evaluation

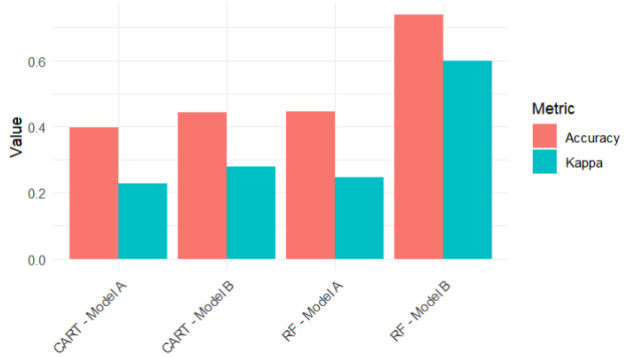

Figure 4. Comparison of Accuracy and Kappa Between Models

The classification performance of the models was evaluated using two standard metrics: overall accuracy and Cohen's kappa coefficient. **Figure 4** illustrates a comparison between the CART and Random Forest algorithms using two input strategies: single-pixel values (Model A) and aggregated zonal statistics (Model B). In terms of accuracy, Random Forest Model B achieved the highest result (0.7374), followed by Random Forest Model A (0.4450), CART Model B (0.4426), and CART Model A (0.3973).

This trend suggests that the Random Forest algorithm outperforms CART in both input scenarios. Additionally, both models performed better when using zonal statistics (Model B) compared to single pixel values (Model A), highlighting the importance of spatial aggregation in improving classification reliability. The same pattern is observed in kappa values, which account for agreement beyond chance. Random Forest Model B again achieved the best result (0.5999), classified as moderate to substantial agreement. CART and RF under Model A settings showed lower kappa values (0.2280 and 0.2460, respectively), indicating poorer classification consistency, particularly in the presence of class imbalance. These findings confirm that combining Random Forest with zonal statistics significantly enhances both the accuracy and robustness of land use classification models. Zonal statistics likely contribute to this improvement by reducing noise and representing more consistent spectral features within each land use unit.

3.4 Class-wise Performance Evaluation

To complement the overall accuracy and kappa metrics, a class-wise evaluation was conducted using precision, recall, and F1-score to assess the classification performance for each land use category. This approach provides a more detailed understanding of how well individual classes were identified by the best performing model, Random Forest Model B.

Table 3. Precision, Recall, and F1-Score per Land Use Class (Random Forest - Model B)

Land Use Class	Precision	Recall	F1-Score
Forest	0.4257	0.7000	0.5294
Cropland	0.1029	0.1546	0.1236
Grassland	0.1056	0.1863	0.1348
Water Bodies	0.7879	0.8667	0.8254
Plantation	0.5685	0.5291	0.5481
Settlement	0.9022	0.8995	0.9008
Rice Field	0.7077	0.6013	0.6502
Shrubland	0.1858	0.2764	0.2222

Table 3 presents the class-wise evaluation of the Random Forest Model B using three standard performance metrics: precision, recall, and F1-score. These metrics provide deeper insight into how accurately and consistently each land use class was predicted by the model. Settlement class achieved the highest overall performance, with a precision of 0.9022, recall of 0.8995, and an F1-score of 0.9008. Similarly, the water bodies class was also well-classified, achieving an F1-score of 0.8254. These results indicate that the model was highly effective in identifying spectrally distinct and spatially dominant classes, particularly settlement areas, which constituted more than 50% of the training data. The overrepresentation of this class likely contributed to the model's ability to generalize its patterns with high consistency. Rice field class, another dominant category, showed

strong classification performance with an F1-score of 0.6502. The model successfully captured the majority of rice field areas, though a moderate number of instances were misclassified, as reflected in its recall value of 0.6013. Plantation and forest classes demonstrated moderate performance, with F1-scores of 0.5481 and 0.5294, respectively.

These results suggest that while the model could identify these vegetated classes reasonably well, some confusion with spectrally similar types especially when mixed within a single polygon may have occurred. In contrast, minority classes such as cropland, grassland, and shrubland exhibited significantly lower F1-scores (0.1236, 0.1348, and 0.2222, respectively). These classes were underrepresented in the training data, and their spectral characteristics often overlapped with other vegetation types. This combination of class imbalance and spectral ambiguity reduced the model's ability to differentiate them clearly.

Importantly, the use of zonal statistics in Model B played a crucial role in improving classification performance especially for spatially coherent classes. By aggregating spectral index values (NDVI, NDBI, and MNDWI) over each land use polygon, zonal statistics reduced within-class spectral variability and mitigated the effects of pixel-level noise. This approach enhanced the model's ability to capture consistent patterns across land use classes, which likely contributed to the superior performance of Random Forest Model B compared to models based solely on individual pixel values.

These findings are in line with previous studies that have shown improvements in land use classification accuracy when spatial aggregation techniques are combined with ensemble learning algorithms **[11]**, **[12]**, **[19]**. Likewise, several studies have reported that applying zonal statistics or object-based image analysis (OBIA) helps reduce spectral noise and improve the separability between land use classes **[7]**, **[11]**, **[12]**. Consistent with those findings, this study demonstrates that incorporating zonal-level spectral indicators enhances the stability of class identification and increases the robustness of the Random Forest model.

Overall, the results highlight that integrating zonal statistics with a robust classification algorithm such as Random Forest not only improves overall classification accuracy but also strengthens the reliability of dominant land use categories. Nevertheless, challenges remain in accurately identifying minority and spectrally mixed land use types, emphasizing the need for detailed, class-level assessments in future land use classification research.

Commented [L4]: Add an explanation of how the results of this study relate to previous relevant studies.

4. CONCLUSION

This study demonstrates that the integration of zonal statistics with supervised machine learning, particularly the Random Forest algorithm, significantly enhances the accuracy and robustness of land use classification from Sentinel-2 imagery. By aggregating spectral indices such as NDVI, NDBI, and MNDWI within each land use polygon, zonal statistics reduce pixel-level noise and improve feature consistency, resulting in better performance compared to pixel-based methods. Among the evaluated models, Random Forest using zonal features (Model B) achieved the highest performance, with an overall accuracy of 73.74% and a kappa coefficient of 0.5999. Class-wise analysis further confirmed its effectiveness, particularly in dominant and spectrally distinct classes like settlement, water bodies, and rice fields. However, the model struggled to accurately classify underrepresented and spectrally similar classes such as cropland, grassland, and shrubland, which can largely be attributed to class imbalance in the training data. To

address this limitation, future research should consider implementing data balancing techniques such as oversampling, undersampling, or class-weighted models. Incorporating additional input features, such as texture, elevation, or time-series indices, may also help distinguish spectrally overlapping classes. Furthermore, higher-resolution imagery and the adoption of more advanced methods, including deep learning or hybrid architectures, could offer further improvements. The inclusion of more detailed field validation data is also recommended to enhance model reliability and support more balanced representation across all land use classes.

FUNDING INFORMATION

Authors state no funding involved.

AUTHOR CONTRIBUTIONS STATEMENT

I Gede Awantara : Conceptualization, methodology, data curation, formal analysis, software, visualization, writing original draft. Kusman Sadik : Supervision, conceptual validation, writing, reviewing, and editing. Cici Suhaeni : Methodology, validation, technical review, and reviewing. Agus Mohamad Soleh : Supervision, validation, final review, and editing.

CONFLICT OF INTEREST STATEMENT

Authors state no conflict of interest.

INFORMED CONSENT

This study did not involve human participants, and therefore informed consent was not required

ETHICAL APPROVAL

This study did not involve human participants or animals. Therefore, ethical approval was not required.

DATA AVAILABILITY

The data that support the findings of this study are publicly available. Land use class data were obtained from the Geospatial Information Agency https://tanahair.indonesia.go.id and satellite imagery data were obtained from the Sentinel-2 Level 2A dataset provided by the Copernicus Open Access Hub https://dataspace.copernicus.eu. All data used in this research are open access and can be freely downloaded from the respective sources.

REFERENCES

[1] T. Hermosilla, M. A. Wulder, J. C. White, and N. C. Coops, "Land cover classification in an era of big and open data: Optimizing localized implementation and training data selection to improve mapping outcomes," *Remote Sens Environ*, vol. 268, p. 112780, 2022, doi: https://doi.org/10.1016/j.rse.2021.112780.

[2] S. Basheer *et al.*, "Comparison of Land Use Land Cover Classifiers Using Different Satellite Imagery and Machine Learning Techniques," *Remote Sens (Basel)*, vol. 14, no. 19, Oct. 2022, doi: 10.3390/rs14194978.

[3] Y. G. Yuh, W. Tracz, H. D. Matthews, and S. E. Turner, "Application of machine learning approaches for land cover monitoring in northern Cameroon," *Ecol Inform*, vol. 74, May 2023, doi: 10.1016/j.ecoinf.2022.101955.

[4] Q. Zhu *et al.*, "Land-Use/Land-Cover change detection based on a Siamese global learning framework for high spatial resolution remote sensing imagery," *ISPRS Journal of Photogrammetry and Remote Sensing*, vol. 184, pp. 63–78, 2022, doi: https://doi.org/10.1016/j.isprsjprs.2021.12.005.

[5] S. Amini, M. Saber, H. Rabiei-Dastjerdi, and S. Homayouni, "Urban Land Use and Land Cover Change Analysis Using Random Forest Classification of Landsat Time Series," *Remote Sens (Basel)*, vol. 14, no. 11, Jun. 2022, doi: 10.3390/rs14112654.

[6] T. Adugna, W. Xu, and J. Fan, "Comparison of Random Forest and Support Vector Machine Classifiers for Regional Land Cover Mapping Using Coarse Resolution FY-3C Images," *Remote Sens (Basel)*, vol. 14, no. 3, Feb. 2022, doi: 10.3390/rs14030574.

[7] G. Amin, I. Imtiaz, E. Haroon, N. us Saqib, M. I. Shahzad, and M. Nazeer, "Assessment of Machine Learning Algorithms for Land Cover Classification in a Complex Mountainous Landscape," *Journal of Geovisualization and Spatial Analysis*, vol. 8, no. 2, Dec. 2024, doi: 10.1007/s41651-024-00195-z.

[8] L. S. Macarringue, É. L. Bolfe, and P. R. M. Pereira, "Developments in Land Use and Land Cover Classification Techniques in Remote Sensing: A Review," *Journal of Geographic Information System*, vol. 14, no. 01, pp. 1–28, 2022, doi: 10.4236/jgis.2022.141001.

[9] M. Mehmood, A. Shahzad, B. Zafar, A. Shabbir, and N. Ali, "Remote Sensing Image Classification: A Comprehensive Review and Applications," 2022, *Hindawi Limited*. doi: 10.1155/2022/5880959.

[10] S. Winsemius and J. Braaten, "Zonal Statistics," in *Cloud-Based Remote Sensing with Google Earth Engine*, Springer International Publishing, 2024, pp. 463–485. doi: 10.1007/978-3-031-26588-4_24.

[11] S. Singla and A. Eldawy, "Raptor Zonal Statistics: Fully Distributed Zonal Statistics of Big Raster + Vector Data [Pre-Print]," Oct. 2020, [Online]. Available: http://arxiv.org/abs/2010.06641

[12] R. Saldanha *et al.*, "Zonal statistics datasets of climate indicators for Brazilian municipalities," *Environmental Data Science*, vol. 3, 2024, doi: 10.1017/eds.2024.3.

[13] V. C. Radeloff *et al.*, "Need and vision for global medium-resolution Landsat and Sentinel-2 data products," *Remote Sens Environ*, vol. 300, p. 113918, 2024, doi: https://doi.org/10.1016/j.rse.2023.113918.

[14] S. Huang, L. Tang, J. P. Hupy, Y. Wang, and G. Shao, "A commentary review on the use of normalized difference vegetation index (NDVI) in the era of popular remote sensing," Feb. 01, 2021, *Northeast Forestry University*. doi: 10.1007/s11676-020-01155-1.

[15] T. A. Kebede, B. T. Hailu, and K. V. Suryabhagavan, "Evaluation of spectral built-up indices for impervious surface extraction using Sentinel-2A MSI imageries: A case of Addis Ababa city, Ethiopia," *Environmental Challenges*, vol. 8, Aug. 2022, doi: 10.1016/j.envc.2022.100568.

[16] A. Gatti, A. Bertolini, and F. Carriero, "Sentinel-2 Products Specification Document Sentinel-2 Products Specification Document Written by Company Responsibility Date Signature."

[17] O. S. Belhaj, S. Mubako, and W. L. Hargrove, "Determination of Change in Surface Waterbodies in The Middle Rio Grande Basin by Modified Normalized Difference Water Index (MNDWI," 2022. [Online]. Available: https://www.researchgate.net/publication/366865340

[18] N. C. Paul, N. Ponnaganti, K. S. Reddy, and D. D. Nangare, "Modified Normalized Difference Water Index Mapping of Pune District Using Google Earth Engine," *National Academy Science Letters*, 2025, doi: 10.1007/s40009-025-01617-2.

[19] S. Chatterjee, S. C. Murray, F. I. Mattias, and N. Fahlgren, "FIELDimagePy: A tool to estimate zonal statistics from an image, bounded by one or multiple polygons," *Crop Sci*, Jan. 2024, doi: 10.1002/csc2.21357.

[20] M. Bansal, A. Goyal, and A. Choudhary, "A comparative analysis of K-Nearest Neighbor, Genetic, Support Vector Machine, Decision Tree, and Long Short Term Memory algorithms in machine learning," *Decision Analytics Journal*, vol. 3, p. 100071, Jun. 2022, doi: 10.1016/j.dajour.2022.100071.

[21] A. Roy and S. Chakraborty, "Support vector machine in structural reliability analysis: A review," *Reliab Eng Syst Saf*, vol. 233, p. 109126, 2023, doi: https://doi.org/10.1016/j.ress.2023.109126.